

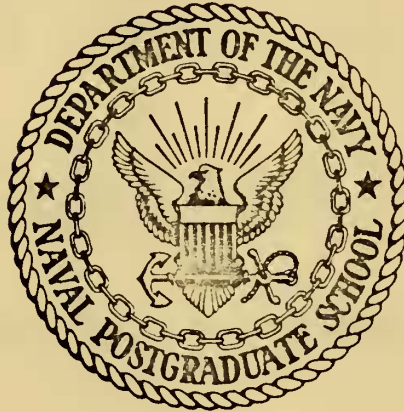
DETERMINATION OF THE DEEP WATER ARRIVAL
DIRECTION OF OCEAN SWELL AT A COASTAL STATION

Marshall Harlan Austin



NAVAL POSTGRADUATE SCHOOL

Monterey, California



THESIS

DETERMINATION OF THE DEEP WATER
ARRIVAL DIRECTION OF OCEAN SWELL AT A COASTAL STATION

by

Marshall Harlan Austin, Jr.

Thesis Advisor:

W. C. Thompson

March 1972

Approved for public release; distribution unlimited.

Determination of the Deep Water
Arrival Direction of Ocean Swell at a Coastal Station

by

Marshall Harlan Austin, Jr.
Lieutenant, United States Navy
B.S., United States Naval Academy, 1964

Submitted in partial fulfillment of the
requirements for the degree of

MASTER OF SCIENCE IN OCEANOGRAPHY

from the

NAVAL POSTGRADUATE SCHOOL
March 1972

ABSTRACT

Three previously unpublished methods for empirically determining deep-water swell direction were examined in this work: (1) triangulation using two widely separated wave sensors, (2) intersection using weather maps and a single wave sensor, and (3) swell point-source estimation from weather maps. The primary objective of each method was to identify a single point source of the swell train produced in an approaching cyclonic storm. Method (1) was not adequately tested, but results as applied to swell from one storm were favorable. Methods (2) and (3), applied to five selected North Pacific storms, gave close agreement on the swell origin time (15 minutes to 6 hours) and source point location (27 to 362 nautical miles), and on swell arrival direction at Monterey, California (0.1 to 5.3 degrees). Methods (1) and (2) give deep-water directions for swell trains that have already arrived, while Method (3) is a prediction method.

TABLE OF CONTENTS

I. INTRODUCTION 7

II. SWELL GENERATION AND PROPAGATION CONSIDERATIONS 11

III. DETERMINATION OF DEEP-WATER SWELL DIRECTION 15

 A. METHOD ONE: TRIANGULATION USING TWO SENSORS 15

 B. METHOD TWO: TRIANGULATION USING WAVE RECORDS
 AND WEATHER MAPS 21

 C. METHOD THREE: PREDICTION FROM WEATHER MAPS 29

IV. COMPARISON OF THE THREE METHODS 37

 A. COMPARISON OF THE THREE METHODS FOR STORM 3 37

 B. COMPARISON OF METHODS TWO AND THREE FOR ALL STORMS 37

LIST OF REFERENCES 43

INITIAL DISTRIBUTION LIST 44

FORM DD 1473 46

LIST OF TABLES

I.	Results of Method Two	28
II.	Results of Method Three	35
III.	Prediction of Time of Peak Swell Arrival at Monterey	36
IV.	Comparison of Results from Methods Two and Three	41
V.	Swell Arrival Direction at Monterey Resulting from 12 and 24 Hour Error in Estimating Time of Origin	42

LIST OF FIGURES

1	Frequency-Time Graph for Storm 4	19
2	Determination of Origin of Peak Swell Generated by Storm 3 Using Method One	20
3	Analysis of Storm 5 Using Method Two	24
4	FNWC Computer-Drawn Surface Pressure Analysis for 00Z 13 Dec 71 Surface Pressure Map	25
5	Wind Profile Along Axis of Peak Winds on 00Z 13 Dec 71 Surface Pressure Map	26
6	Frequency-Time Lines for the Five Storms Studied	27
7	Time of Origin Prediction Graph for Storm 5	33
8	Period and Frequency of Maximum Energy for a Fully Arisen Sea Versus Surface Wind Velocity	34
9	Swell Origin Points for Storm 3 as Determined by Methods One, Two and Three	38

ACKNOWLEDGEMENTS

The author wishes to express his appreciation to the personnel at Fleet Numerical Weather Central, Monterey, California, who provided him with weather maps, digitizing equipment, and use of the CDC 6500 computer facility, all of which were necessary for the accomplishment of this work.

The three methods developed and tested in this thesis, and also the concepts and procedures described under Methods Two and Three to identify the swell source from weather maps, were proposed to the author by W. C. Thompson. To Professor Thompson I give my most sincere thanks for his professional guidance and criticism in helping me to find my way along the path of academic research.

And, finally, to my wife, my gratitude for her understanding, patience and support during the last two years.

I. INTRODUCTION

Deep-water swell direction information is needed for most operational coastal engineering work. Swell direction data, used by coastal engineers for such purposes as the design of structures and the computation of littoral drift, can be found in the form of statistical compilations derived from wave-hindcasting methods. However, the deep-water direction increments used in such compilations are 45 degrees and 22.5 degrees. These direction intervals are crude when the sensitive dependence of refraction on deep-water wave direction is taken into account in computing shoal-water wave data for a selected coastal site. Swell direction, generally in the form of a mean direction, can be obtained from wave forecasting or hindcasting from weather maps, from multiple sensor arrays placed in shoal water, and from more exotic procedures such as sea-glitter measurements and laser profiling from aircraft. The latter methods are not used to obtain operational wave-direction information, and have the disadvantage of being very costly.

In this study three previously undescribed methods for obtaining deep-water swell direction were investigated using recorded wave data from coastal sensors located at Monterey and San Clemente Island, California and synoptic weather maps. The three methods were tested on five selected storms occurring from October through December, 1971 which were tracked across the North Pacific. The swell direction from each storm was determined for deep water directly off Monterey.

The three methods are all based on the concept that the dominant swell observed at a distant location is generated at a point source in space and time. They all involve identification of the point source. Once this

swell source is determined, the swell are then followed at group velocity to the coastal station of interest along a great-circle path, and the azimuth of the path at the coastal site is taken to represent the deep-water arrival direction for the swell train. The single direction that is obtained is considered here to be the direction of the dominant swell arriving at the station. It is recognized that real swell display both a directional and frequency spectrum; however, it is also evident that the size of ocean storms is normally such that for most storms at distances on the order of 1000 nautical miles or greater the directional bandwidth is narrow and sharply peaked. Accordingly, the determined azimuth is considered to represent the dominant band of the arriving directional spectrum with good precision.

In the present study, a point source is thought of as that region of the sea surface (small compared to the travel distance) and that time interval (small compared to the travel time) in which a prominent energy maximum is generated by the storm and from which the energy is then propagated toward the distant station of interest. It is assumed in this work that the swell observed at a distant station then represents the dispersive arrival of a burst of energy imparted to the sea at the source location and time. To identify this point source the three approaches formulated and tested were:

1. Triangulation using swell source distances derived from analysis of the wave records from two coastal sensors at widely separated locations.

2. Use of a single coastal wave sensor and synoptic weather maps. The sensor gives the swell origin distance and time, and the weather maps give a probable path of the point of maximum wave generation toward the coastal station from map to map during the life of the storm. The intersection of the distance arc and the path of maximum wave generation represents the single source point for the swell.

3. Determination of the swell origin point from weather maps, by examining the surface pressure fields, in order to find that set of wind conditions which produces the maximum wave energy directed toward the coastal station.

The North Pacific storms and swell trains, occurring in late 1971, examined in this paper, are indicated as follows:

<u>STORM/SWELL TRAIN NUMBER</u>	<u>STORM OCCURENCE</u>	<u>SWELL ARRIVAL AT MONTEREY</u>
1	25-26 October	30 Oct - 1 Nov
2	31 Oct - 5 Nov	7-9 November
3	19-24 November	25-26 November
4	22-26 November	28-29 November
4A	26-29 November	29 Nov - 1 Dec
5	11-14 December	16-18 December

Storms 1, 2, 3, and 5 were uncomplicated storms that developed and traveled across the North Pacific much in the manner expected of winter storms. Storm 4 presented an analysis problem. After several days of development it weakened considerably and appeared ready to die out. However, the center of the low shifted its position about 420 nautical miles to the southwest over a 12-hour map interval, and the storm

re-intensified. After about 24 hours the storm then moved to the east as normally expected. For this reason, and because spectral analysis of the waves at Monterey indicated two arriving swell trains, it was decided to analyze this particular event as two separate storms, each with a unique source point. The earlier portion of the storm was accordingly labelled Storm 4, and the latter Storm 4A.

II. SWELL GENERATION AND PROPAGATION CONSIDERATIONS

The five cases studied all deal with the moving fetch problem of swell produced in a moving cyclonic storm where the swell is propagated toward a coastal station located approximately in the direction of the storm's advance. In this situation, it is usual for the wave-generating area to travel for a number of hours in the same direction and at the same speed as the group velocity of some of the frequency components produced in the sea. Accordingly, the effective duration of the wind over the waves is long, the maximum amount of energy the prevailing wind can transfer to the sea is transferred, and the sea approaches or reaches a fully arisen condition.

The maximum energy put into the sea during the passage of a storm across the North Pacific, in the case of waves traveling in the direction of the storm, is determined by two factors: (1) the wind speed, and (2) the relative speed of the wave generating area with respect to the speed of the wave energy propagation. It can be expected that in storms where the difference between the speed of the storm and waves is always large, the maximum energy will be put into the waves about the time of maximum winds. On the other hand, the time of maximum energy input into the sea in a moving storm can be expected to occur when the storm speed equals the group velocity of the waves of the peak frequency that can be generated by the wind then blowing, even though the winds may have been stronger at a time when the relative velocity of storm and waves was very different.

During its passage across the North Pacific, the speed of the wave-generating area is usually roughly the same as the group velocity of the longer waves that can be generated by the winds present. It thus appears that the sea generated in the direction of storm travel must reach a fully arisen condition, either when the wind in the storm reaches its peak mean velocity or when the relative speed of the storm and waves is coincident. That time is then the time when the energy in the sea is at a maximum.

One of the fundamental relationships used in this study, both in the analysis of wave records to determine source distance and origin time of arriving swell trains and to predict from weather maps the arrival times and frequencies in a swell train generated in a cyclonic storm, was the frequency-time (f-t) graph introduced by Munk, et al. (1963).

Using spectral analysis of successive wave records, these investigators determined the energy density at selected frequencies and constructed from this information a frequency-time graph showing the spectral energy density distribution by means of contours for the period of time covered by the wave records. These graphs show that a swell train arriving from a storm is revealed as a prominent sloping ridge line in the spectral density topography. For swell from storms at moderate and great distances these ridge lines are linear.

In the context of linear wave theory, a straight f-t line implies a point source for the swell train in both space and time, and provides a simple means for determining the apparent generating point location and origin time. In practical application a point source implies that the linear dimensions of the wave generating area are small compared to swell travel distance and that the source duration is small compared to travel

time. In the present study, swell from source distances as close to the wave recording station as 1970 nautical miles were treated. The swell signatures on the f-t graphs constructed using recorded wave data were linear for these distances, and the source information derived for the swell train was consistent with the weather maps. It may be noted here that Snodgrass, et al. (1966) dealt with swell sources at distances as small as 1320 nautical miles.

The distance and origin time of the swell source with respect to the wave sensor can be obtained from the f-t curve fitted to the swell data in the following way. If the energy associated with each frequency component, f , generated in the sea is propagated at its own group velocity, C_g , over a distance, D , from the generating point to the observation point in travel time, $t-t_0$, then

$$C_g = D/(t-t_0)$$

but

$$C_g = g/4\pi f$$

from linear wave theory, so that

$$g/4\pi f = D/(t-t_0).$$

The slope of the f-t line is then

$$df/dt = g/4\pi D.$$

Therefore, the apparent distance from the estimated source point is given by

$$D = 1.515/(df/dt) \quad \text{nautical miles} \quad (1)$$

where f is in Hertz and t is in hours. The estimated origin time, t_0 , is given by the intercept of the f-t curve with the zero frequency line.

Equation (1) assumes that the distance, D , between the source and observation point is constant. If this were not the case, there would be an additional term in Equation (1) to account for the change in slope of the f - t curve as the storm moves across the ocean. The assumption of Munk, et al. (1963) that the f - t curve is linear is interpreted in this thesis to mean that the energy is impulsively transmitted to the waves at the space-time point-source; therefore, the distance of swell propagation to a distant station may be considered constant for this burst of energy.

The specific applications of the f - t graph in this study will be shown later.

III. DETERMINATION OF DEEP-WATER SWELL DIRECTION

A. METHOD ONE: TRIANGULATION USING TWO SENSORS

This method involved triangulation to determine the swell source point using data obtained from spectrally analyzed wave records of a given swell train recorded at two widely separated coastal wave sensors. The source point was located by striking arcs of great-circle distance from each sensor site, the radii of which equal the swell source distances as derived from the f-t curve for each station.

The original plan was to use the wave gages at San Clemente Island, California and Newport, Oregon, which are about 700 nautical miles apart; however, failure of the Newport sensor cable precluded its use. The Monterey gage was chosen as an alternate sensor. This choice reduced the wave-gage separation to about 300 nautical miles. It also placed the Monterey and San Clemente Island sensors roughly on a line with the swell source point to be located, thereby reducing the intersection angle between the two radii to a small value. Because of this unsatisfactory triangulation geometry, this method was applied to the swell from one storm only. Storm 3 was chosen because of its high winds and uncomplicated character.

1. Wave Recording and Spectral Analysis

The arriving waves at Monterey were recorded by a Marine Advisers Model A-2 pressure sensor located in 28 feet (MWL) of water off Del Monte Beach. Waves arriving at San Clemente Island were recorded on a pressure sensor located near the northwestern tip of the island in 40 feet (MWL) of water. This sensor is maintained and operated by the Fleet Weather

Facility, San Diego, California. The waves at both gages were recorded in analog form on a paper strip chart. The records consisted of a twenty-minute fast trace every six hours recorded at a chart speed of one inch in 30 seconds, separated by a slow trace.

The consecutive twenty-minute fast traces for the duration of the swell train at both stations were first converted from analog form to digital data using a Calma Company digitizer made available by the Fleet Numerical Weather Central (FNWC), Monterey, California. This taped information was transferred to punched cards using the program CONVERT (Lynch, 1970) designed for use in the FNWC CDC 6500 computer.

A frequency spectrum analysis was then performed on the digitized wave record using the Blackman-Tukey (1958) method. As evidenced by the spectra produced, the highest wave frequency measured was about 0.20 Hz; accordingly, the number of degrees of freedom was 14.5 and the 90 percent confidence limits were 0.60 and 2.10 of the energy density estimates for the width of spectral bands chosen. The output of the analysis was wave frequency (Hertz) and the corresponding energy density (feet²-second) in both tabular and graphical forms. The energy values were computed for frequencies from 0.0 to approximately 0.24 Hz, in 0.00416 Hz increments.

2. Determination of Swell Source Distance and Origin Time

The spectral energy density at six-hourly intervals during the period of swell arrival was plotted on a frequency-time graph for each station. An f-t line was then fitted to the spectral energy peaks. From the slope of the f-t curve the distance to the point of origin was determined, and from its intercept with the zero frequency axis the time of origin was determined, as explained above. The frequency-time graph of spectral energy density for Swell Train 4 is shown in Figure 1.

It is possible for the frequency of maximum energy density in swell to shift across the spectrum due to shoaling effects as the waves travel from deep to shallow water. Thompson (1970) investigated this phenomenon and determined that the magnitude of a frequency shift of this sort is negligible for swell passing over a narrow coastal shelf.

3. Great-Circle Distance and Trajectory Overlays

In order to quickly and easily measure great-circle distances on the weather maps, to determine the trajectory from the swell source to the station, and to measure the arrival direction of swell at the station, a computer program was written using a Naval Research Laboratory subroutine titled TO-NRL-GCDIST (Chang, 1969). The program produced a tabulation of great-circle distances and the azimuths of these great-circles from Monterey and San Clemente Island to integer latitude-longitude intersections (one-degree increments) in the North Pacific Ocean. Using this table, two very convenient transparent overlays were drawn for each station for use on the FNWC strip chart of the North Pacific Ocean (1:30 million-scale polar stereographic projection). The first of these overlays contains a family of arcs of great-circle distance in 100 nautical-mile increments, while the second shows great-circle paths drawn for five-degree increments of arrival direction at the station. Distance overlays were drawn for Monterey and San Clemente Island. These overlays and the associated table were used extensively throughout this investigation.

4. Application of Method One

As mentioned above, this method was applied only to Swell Train 3, which was observed to arrive at the two coastal stations on 25-26 November, 1971.

The source distances and origin times obtained from the f-t curves drawn from the swell data at the two stations are as follows:

<u>Station</u>	<u>Source Distance</u>	<u>Origin Time</u>
MRY	2330 naut mi	03Z/21 Nov 71
SCI	2640 naut mi	00Z/21 Nov 71

Triangulation was performed by constructing arcs from both gages at their respective source distances on a base map using the distance overlays. These arcs are shown in Figure 2.

Triangulation cannot be performed directly using these arc distances because the origin times are not coincident. In order to resolve this problem one of the sets of data was accepted as a reference, namely that for the Monterey gage. The data from the San Clemente Island gage were then adjusted as follows. Three hours were added to the origin time for the swell arriving at San Clemente Island to make it coincident with that at Monterey. This time adjustment represents a closer swell source for the San Clemente Island site than was obtained from the f-t graph in an amount given by the distance waves would travel from the source in three hours. Because many frequencies are generated by the storm, each of which travels at a different group velocity, the frequency of maximum energy density in the swell arriving at San Clemente Island ($f_{\max} = 0.07$ Hz)

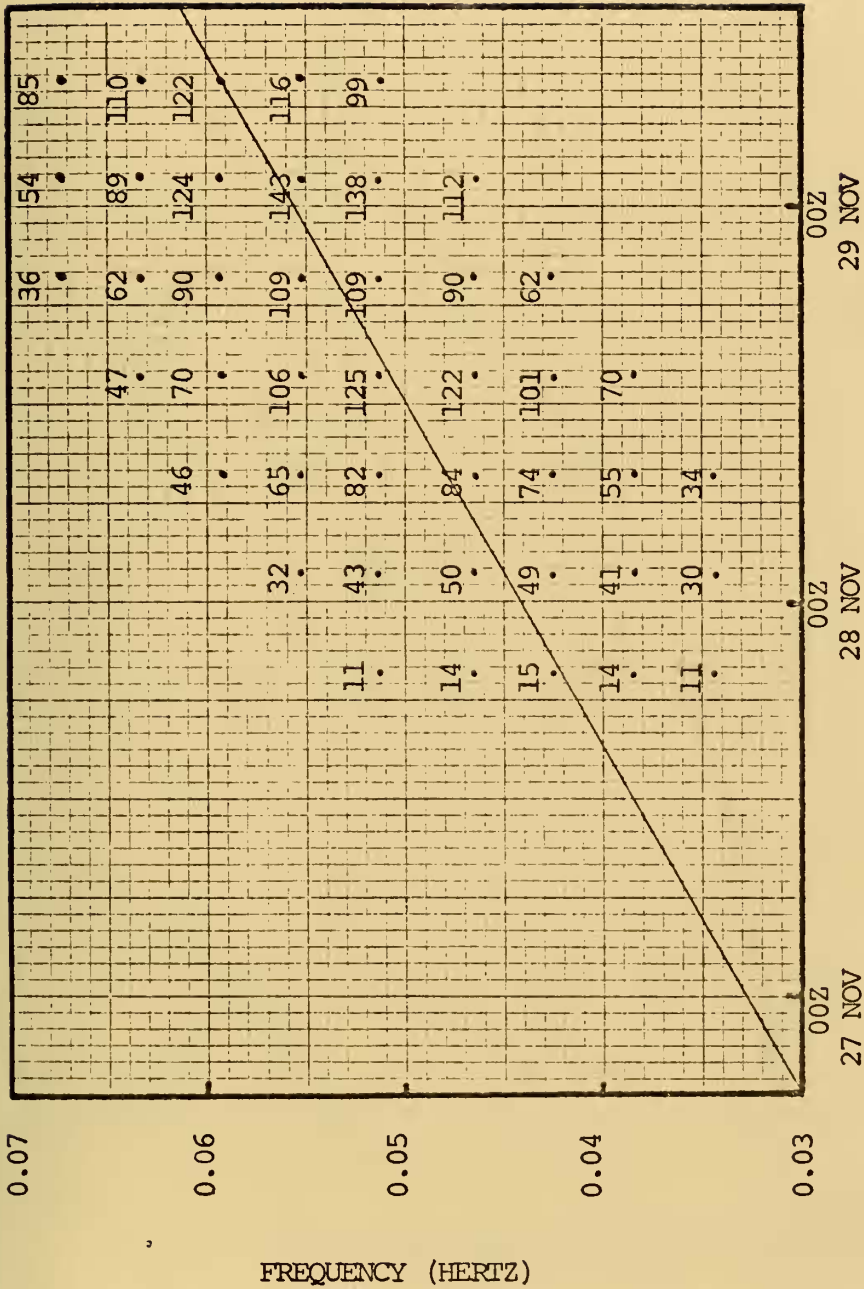


Figure 1: FREQUENCY-TIME GRAPH FOR STORM 4.

Numbers on graph indicate relative energy for f-t points indicated by dots. This figure is representative of a larger graph used in the actual data analysis.

was used to give a representative travel distance. Thus, the travel distance for the three-hour increment, Δt , is:

$$D = C_g \Delta t = \frac{1.515 \Delta t}{f} = 66 \text{ nautical miles.}$$

The adjusted swell source distance from San Clemente Island is then $2640 - 66 = 2574$ nautical miles. This adjusted distance is shown in Figure 2 by the dashed line.

Because the gages at the two stations are nearly in line with the swell source, as is evident from the figure, a satisfactory intersection angle between the two arcs could not be obtained. However, the generally good source distance agreement between the dashed arc drawn from the San Clemente Island gage site and the solid arc drawn from the Monterey site is apparent, and was found to agree with a storm location on the weather maps, as discussed later.

B. METHOD TWO: TRIANGULATION USING WAVE RECORDS AND WEATHER MAPS

1. Procedure

The second method for computing the deep-water swell direction involves determination of the point of swell origin within the storm using the intersection of a swell source distance arc as determined by analysis of the wave records from a coastal wave sensor with the path of the peak winds (defined below) directed toward the sensor site as obtained from analysis of a series of synoptic weather maps. The swell arrival direction is then determined from the great-circle trajectory drawn from the intersection point to a coastal site at or in the vicinity of the wave gage.

The distance from the wave gage to the origin point of the swell is determined from the f-t curve for the swell train by the procedure described under Method One. This distance is then struck as an arc from the sensor site on a blank weather map used for plotting of the data.

The maximum wave energy generated by the storm in the direction of the wave-gage site is considered to be that generated along the peak wind path. The path of maximum surface wind speed directed toward the wave gage site was obtained as follows:

For a given storm, the path of peak winds directed toward the wave-gage site was obtained by plotting the peak wind point derived from each surface pressure analysis onto the blank data map, and then connecting these points of maximum surface winds directed toward the station as is shown in Figure 3. The point of effective maximum winds on an individual weather map was obtained by overlaying on the map the great-circle path template for the Monterey gage, then by using a second transparent template indicating a fifteen degree cross-isobar surface wind flow, locate the axis of the storm along which the surface winds blow 15 degrees across the isobars and directly toward Monterey. A constant fifteen-degree cross-isobar flow angle for the surface wind was chosen as an average value based on common usage. A four-millibar isobar spacing, chosen to give the maximum wind speed, was then measured along this axis and converted to the geostrophic wind velocity, V_g . The point of maximum wind velocity on the axis was considered to represent the source of maximum wave energy being generated on that map in the direction of Monterey. The point of maximum wind speed on each weather map obtained in this way was then connected to produce the path of peak winds for the storm.

In complicated wind fields, wave energy that is directed toward the station from locations off the peak wind axis may represent the maximum energy contributed from a given weather map. This would lead to distances and origin times somewhat different from that obtained from this procedure.

2. Example of Method Two Application

Storm 5 is presented as an example of the procedures used in Method Two. This particular storm was first noted on the weather maps of 11 December 1971, and the first significant swell arrival at Monterey from wave record analysis was on 16 December 1971.

Figure 4 shows the FNC surface pressure map for 00Z 13 Dec 71 analyzed to show the axis of the surface winds in the storm that are blowing 15° across the isobars and directly toward Monterey. The circle represents the point of maximum winds on this axis, and the cross the center of the low-pressure system. The dashed line represents that portion of the axis which lies over and to the north of the Aleutian Island chain, and along which waves generated will not reach Monterey. The wind profile along the axis shown in Figure 4, which is typical of the storms studied, is shown in Figure 5.

Figure 3 shows the axes of winds blowing toward Monterey as analyzed from eight successive 12-hourly surface weather maps. The circled points on the axes represent the points of maximum winds on each map, and are connected to give the path of maximum winds. On this map, the great-circle distance arc (heavy dashed line) is drawn at a distance of 2177 nautical miles, as computed from the f-t diagram for Swell Train Five. The intersection of the distance arc and the path of maximum surface winds (large circle) marks the presumed swell source point. The

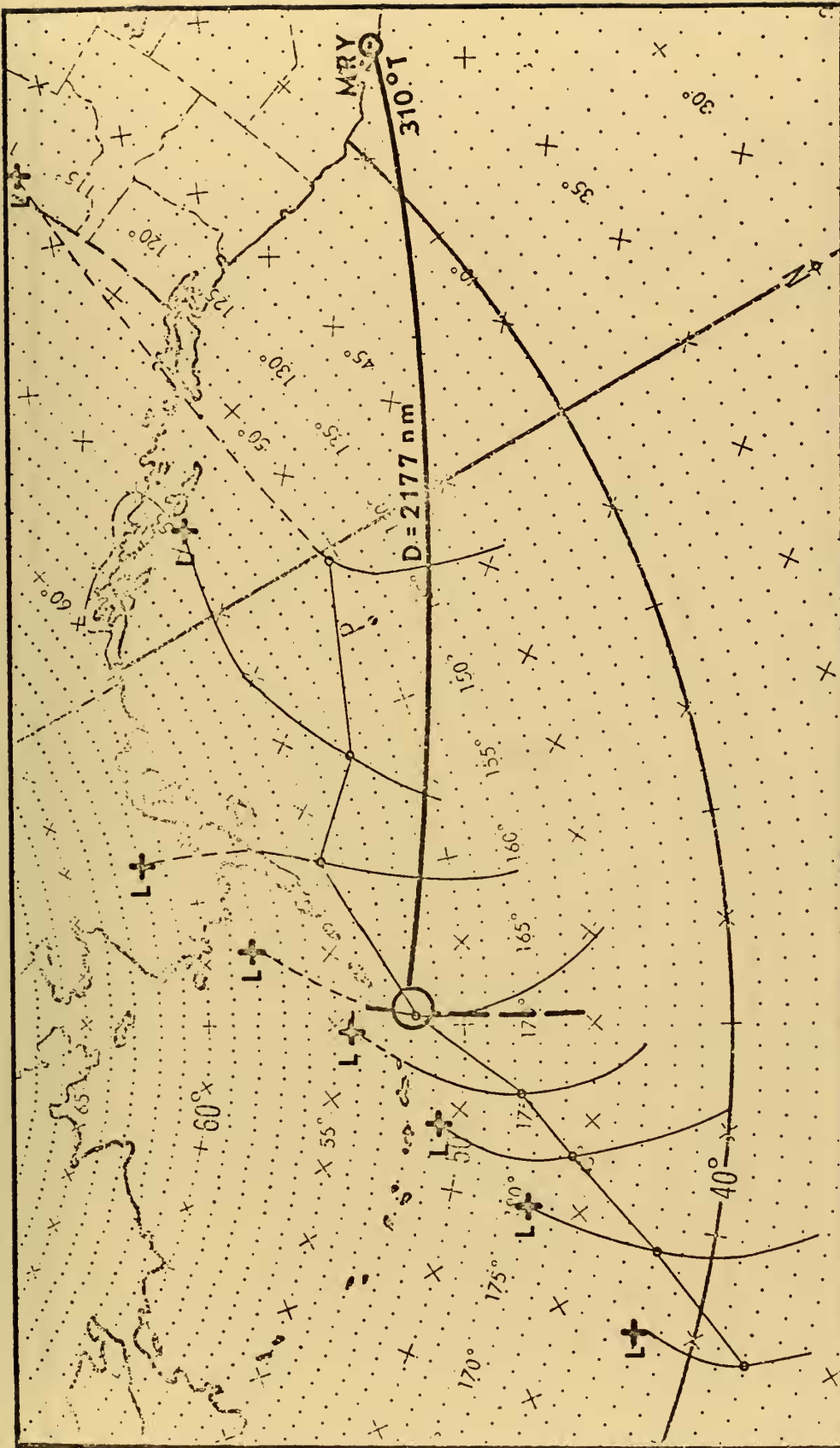


Figure 3: ANALYSIS OF STORM 5 USING METHOD TWO.

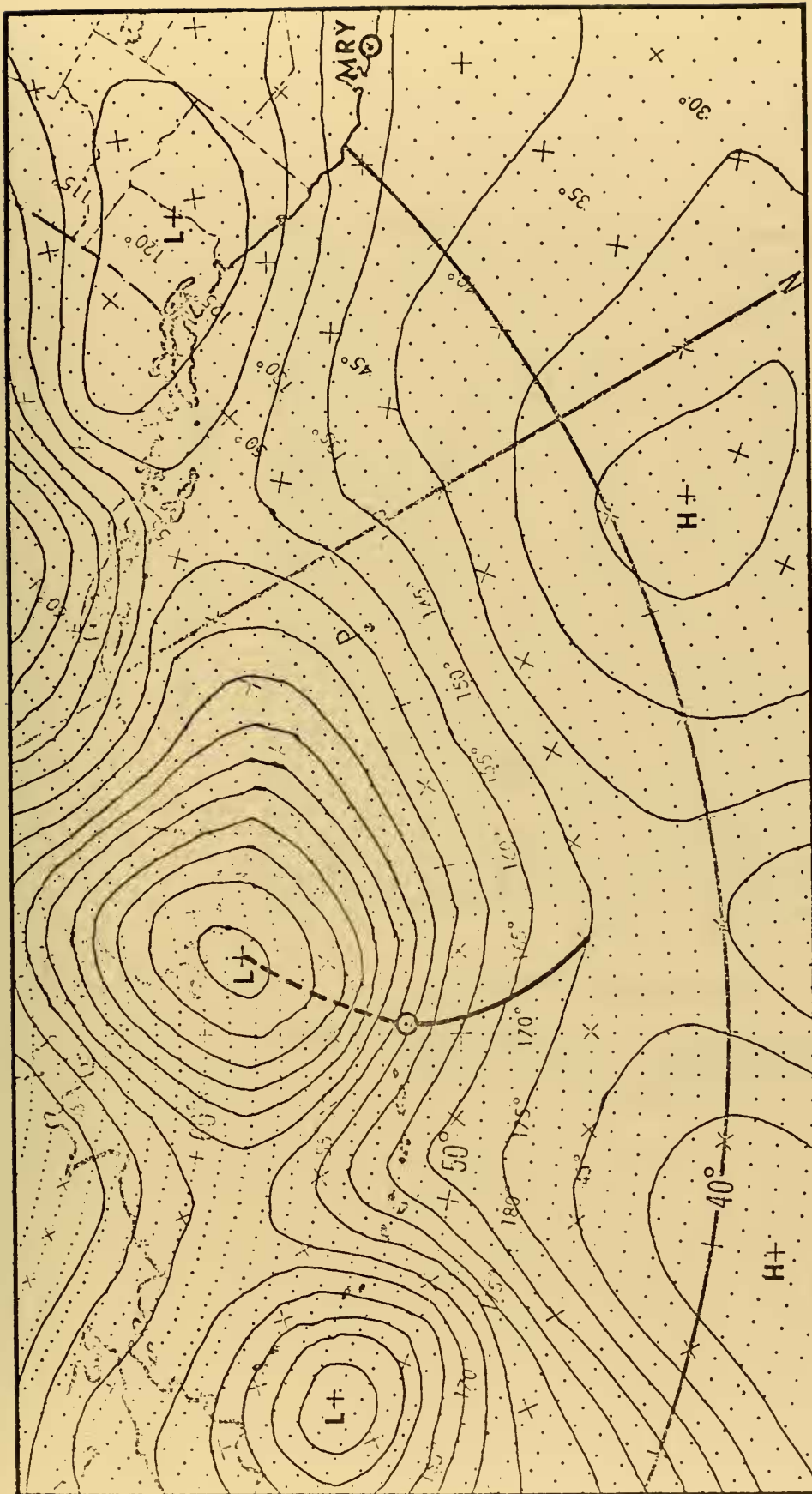


Figure 4: FNWC COMPUTER-DRAWN SURFACE PRESSURE ANALYSIS FOR 00Z 13 DEC 71 SHOWING AXIS OF PEAK WINDS.

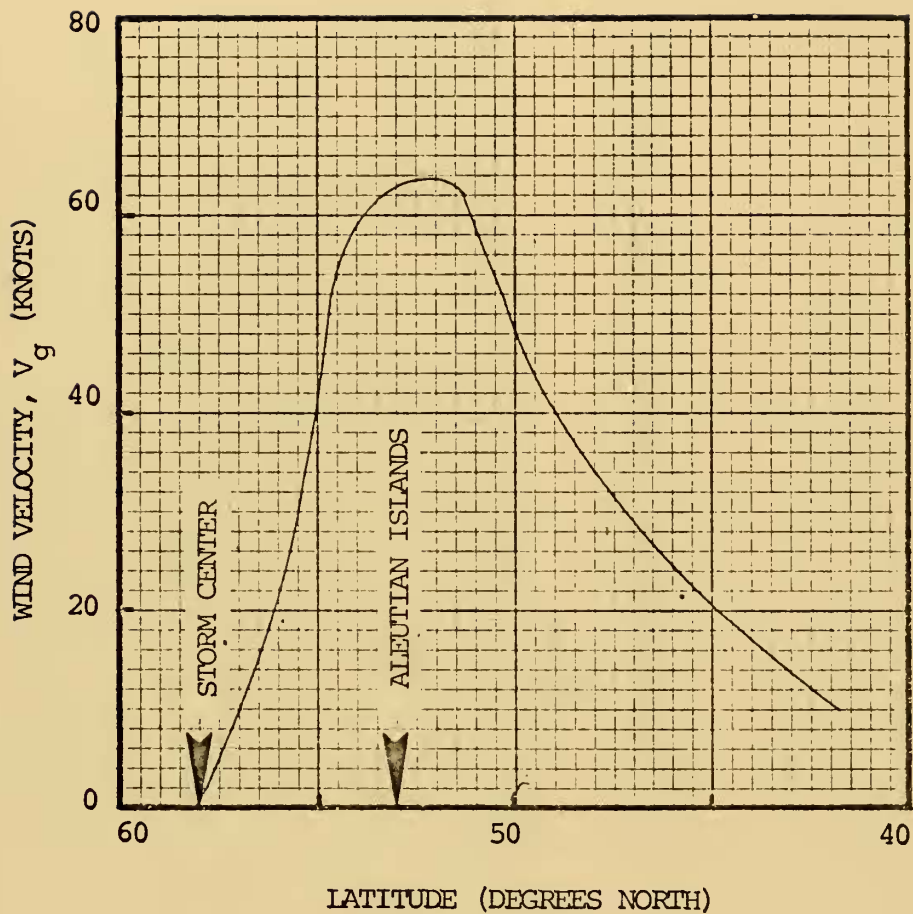
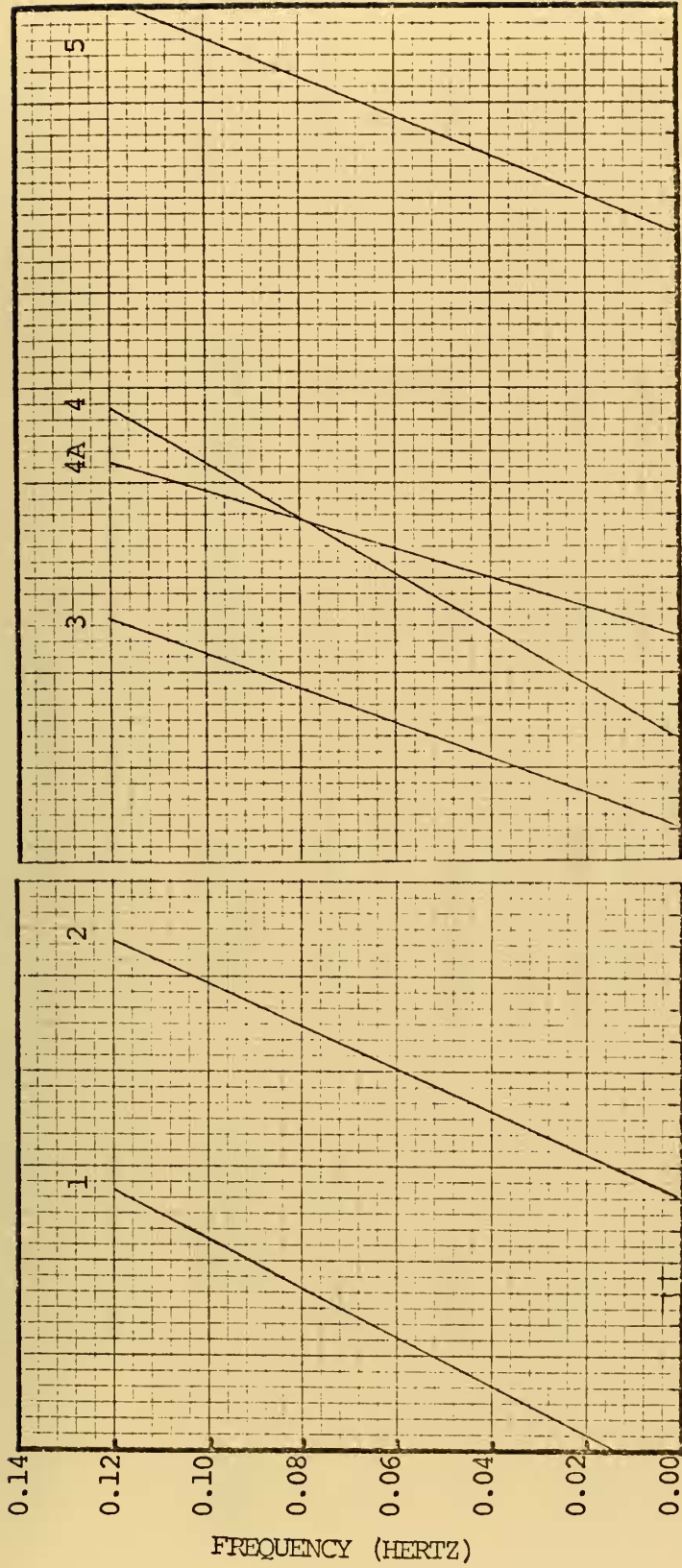


Figure 5: WIND PROFILE ALONG AXIS OF PEAK WINDS
ON 00Z 13 DEC 71 SURFACE PRESSURE MAP.
(Storm 5)



20
DEC

14/23
NOV

27
OCT

Figure 6: FREQUENCY-TIME LINES FOR THE FIVE STORMS STUDIED.

Table I: RESULTS OF METHOD TWO

Swell source distance and origin time from wave record analysis.

<u>Storm Number</u>	<u>Distance From Monterey</u>	<u>Peak Swell Origin Time</u>	<u>Location of Source Point Latitude</u>	<u>Longitude</u>	<u>Arrival Direction at Monterey</u>
1	3010 naut. mi.	1500Z 25 Oct 71	49.0N	169.0E	307.3 °T
2	2220	0600Z 4 Nov 71	51.0N	170.5W	308.5
3	2330	0330Z 21 Nov 71	37.5N	171.0W	286.5
4	3082	0000Z 24 Nov 71	44.5N	169.5E	301.0
4A	2200	2015Z 26 Nov 71	36.0N	168.0W	283.2
5	2177	0115Z 13 Dec 71	52.0N	169.0W	310.3

great-circle propagation path of the swell of peak energy from the source point to Monterey is shown by the heavy solid line. The deep-water arrival direction at Monterey is from an azimuth of 310 degrees (true).

3. Results of Method Two

The results of this method of locating the point source and determining the swell arrival direction for all five storms are presented in Table I. Additionally, Figure 6 shows the f-t curves derived for each of the five storms studied.

C. METHOD THREE: PREDICTION FROM WEATHER MAPS

Method Three is an empirical approach to identification of those events in a storm history which will allow a forecaster to predict accurately the desired swell arrival information. This method uses surface pressure analysis weather maps to estimate the time and point of swell origin, and hence the arrival direction of the peak swell energy at a selected coastal station. The peak swell is that swell which is considered to be produced at the space-time point source by the impulsive introduction of energy into the sea.

Additionally, a useful extension of the data obtained using this method allows one to predict the time of arrival of the peak swell at the station.

1. Time of Origin and Source Point of the Peak Swell

The principal task in the analysis is to identify the time of origin and associated source point of the swell of maximum energy produced by the storm that is directed toward the coastal station. The individual weather maps showing the storm of interest are examined, and their peak wind points are plotted on a blank base map, as outlined in Method Two (illustrated in Figure 3). The connected path of points of peak wind

velocity then represents the locus of possible peak-swell origin points for that storm. To determine the swell origin point on the path of peak winds, one must next estimate the moment in the storm history when the maximum amount of energy was imparted to the sea. In this work it was assumed that, in the absence of obvious overriding conditions such as higher velocity surface winds at an earlier time with little or no storm movement, the time of origin of the peak swell (and of a fully arisen sea condition) is that time when the group velocity, C_g , of that frequency component of maximum energy that can be produced in a fully arisen sea by the winds present equals the velocity component, V_{GP} , of the peak wind toward Monterey.

A graph showing the history of C_g and V_{GP} with time was prepared for each storm, as shown in Figure 7 for Storm 5. That moment when $C_g = V_{GP}$ is considered to be the source time. It may be seen in Figure 7 that this condition is met on both 11 and 13 December. The 13 December time was considered to be the most probable origin time because of the slightly stronger surface winds and closer approach of the storm to Monterey at that time. Once the moment in the storm's history when C_g and V_{GP} were equal was determined, the location of the point source was established on the path of possible points on the base map by interpolation.

Once the swell source has been chosen, the deep-water arrival direction of the swell is found by use of either the transparent great-circle path overlay or the associated table of values.

The procedures for obtaining V_{GP} and C_g are outlined as follows:

- (1) The velocity component, V_{GP} , of the source point toward the observation station is obtained by dividing the difference in the great-circle distance from the peak wind points on successive weather maps to Monterey

by the time interval between the maps. (2) The group velocity, C_g , of the component of maximum energy is obtained from the geostrophic wind velocity. The geostrophic wind velocity, V_g , for the peak wind point is obtained from the pressure gradient on each surface pressure map. This, in turn, is converted to the surface wind velocity, V_s , using an empirically derived ratio of $V_s/V_g = 0.66$. This constant is for conversion of geostrophic wind velocities obtained using a four-millibar isobar spacing (discussed under Method Two). Assuming that fully arisen sea conditions exist on all maps, the frequency on maximum energy, f_{\max} , produced by the surface wind on each map was obtained from Figure 8 (the construction of this figure is based on the Pierson-Moskowitz (1964) spectrum). The group velocity of the frequency component of maximum energy is then found from the propagation equation, $C_g = 1.515/f_{\max}$ (knots).

The ratio of $V_s/V_g = 0.66$ was determined by the following procedure: The single frequency of maximum energy density for each swell train recorded at Monterey was read from the f-t curves drawn for each swell train as described in Method One. This frequency was converted to V_s for fully arisen sea conditions using Figure 8. The geostrophic wind velocity at each storm's swell origin point determined by Method Two was obtained from the weather maps. The ratio V_s/V_g was then formed for each storm. This set of six values was averaged to obtain the V_s/V_g ratio used in this work.

2. Results

Table II presents the results of the procedures followed in Method Three to determine the origin and the arrival direction at Monterey of the swell trains generated in the five storms studied.

3. Time of Arrival of the Peak Energy Swell

If one assumes that the frequency of the maximum energy swell is conserved, the time of arrival, t , of the swell peak at a distant station can be estimated using

$$t - t_0 = \frac{D}{C_g}$$

where C_g is the group velocity of the frequency component of maximum energy, f_{\max} , produced by the surface wind at the peak wind point.

The results of arrival-time predictions for Monterey obtained in this manner for the six swell trains, along with the time of arrival of the energy peak as determined from spectral analysis of the waves recorded at Monterey, are presented in Table III.

The method tested here is based on an unpublished technique for forecasting ocean swell being developed by W. C. Thompson under FNWC sponsorship.

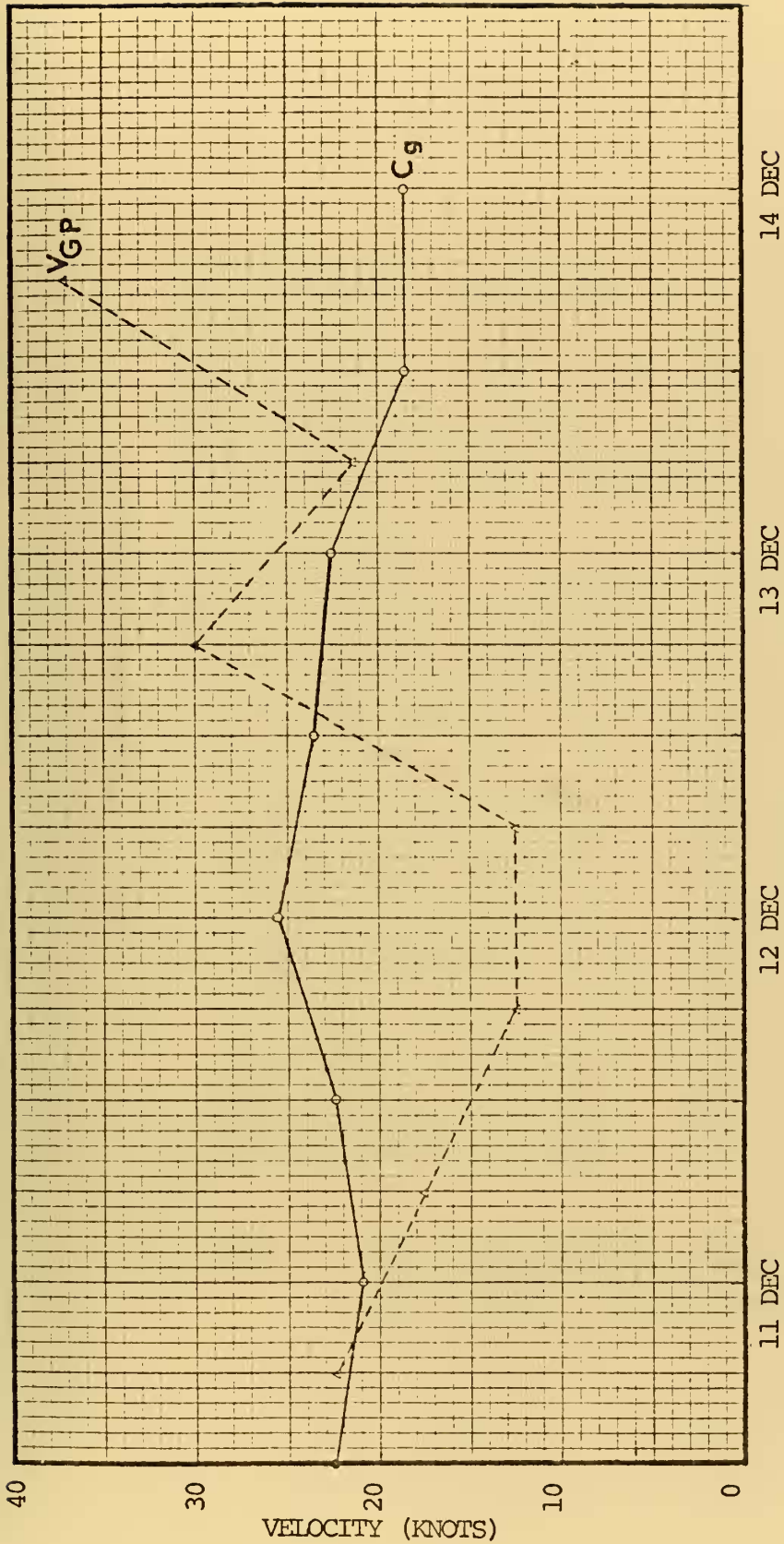


Figure 7: TIME OF ORIGIN PREDICTION GRAPH FOR STORM 5.

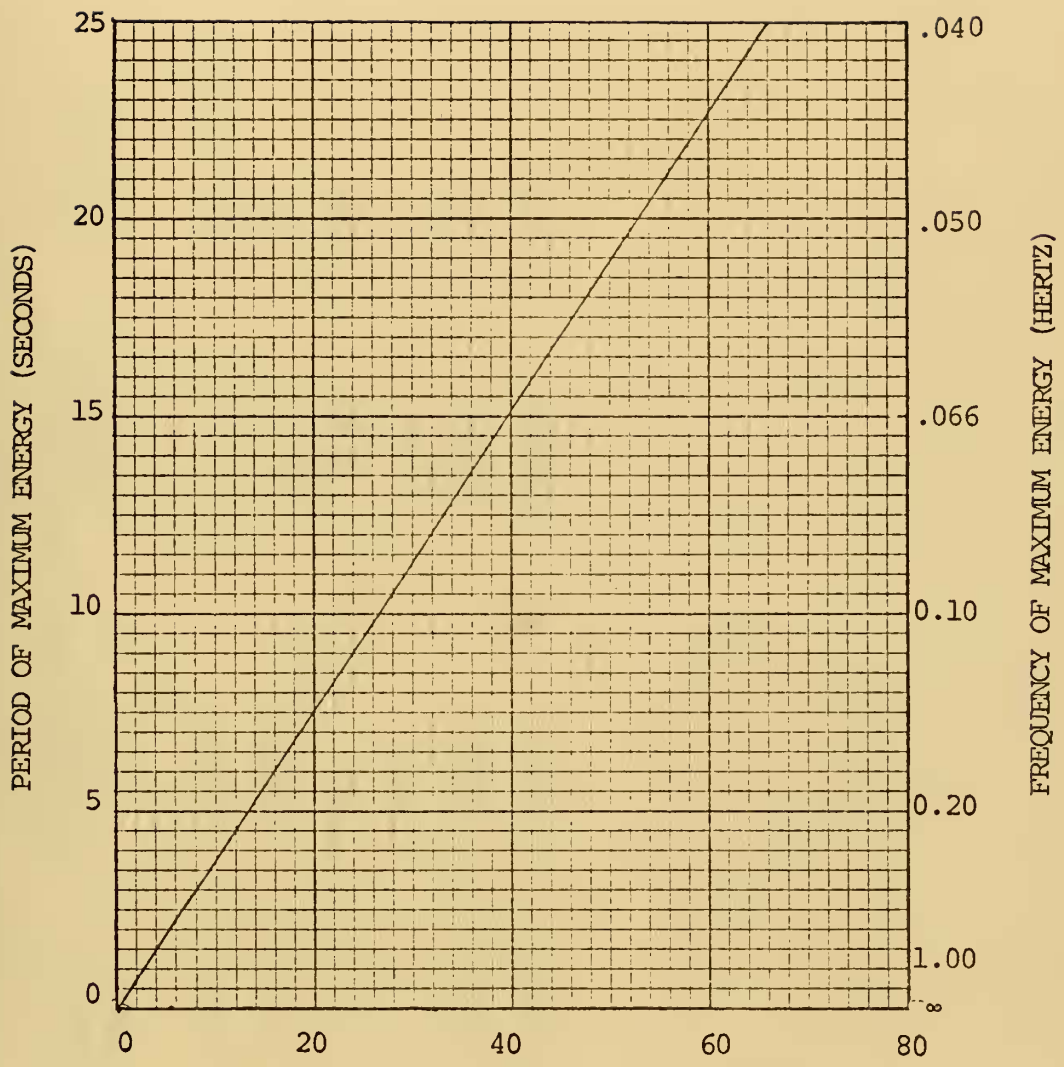


Figure 8: PERIOD AND FREQUENCY OF MAXIMUM ENERGY FOR A FULLY ARISEN SEA VERSUS SURFACE WIND VELOCITY. (After Pierson and Moskowitz, 1964)

Table II: RESULTS OF METHOD THREE

<u>Storm Number</u>	<u>Estimated Time of Origin of Peak Swell</u>	<u>Estimated Source Point Latitude</u>	<u>Estimated Source Point Longitude</u>	<u>Estimated Distance</u>	<u>Arrival Direction at Monterey</u>
1	1900Z 25 Oct 71	49.0N	172.0E	2907 naut. mi.	306.7 °T
2	1200Z 4 Nov 71	49.0N	174.0E	2360	305.2
3	0600Z 21 Nov 71	37.3N	169.0W	2240	285.2
4	2100Z 23 Nov 71	44.0N	173.0E	2935	300.0
4A	0000Z 27 Nov 71	40.5N	161.0W	1838	288.5
5	0130Z 13 Dec 71	52.3N	168.3W	2140	310.4

Table III: PREDICTION OF TIME OF PEAK SWELL ARRIVAL AT MONTEREY

<u>Storm Number</u>	<u>Time of Arrival From Wave Records</u>	<u>Time of Arrival Predicted From Weather Maps</u>	<u>Time Difference (Hours)</u>
1	0800Z 1 Nov 71	0400Z 1 Nov 71	4
2	1930Z 8 Nov 71	0700Z 9 Nov 71	11.5
3	1400Z 24 Nov 71	1600Z 24 Nov 71	2
4	1400Z 28 Nov 71	2330Z 28 Nov 71	9.5
4A	0200Z 30 Nov 71	1900Z 29 Nov 71	7
5	2300Z 16 Dec 71	2330Z 16 Dec 71	0.5

IV. COMPARISON OF THE THREE METHODS

A. COMPARISON OF THE THREE METHODS FOR STORM THREE

As explained in the discussion of Method One, Storm 3 was the only storm on which all three methods were tested. The peak swell origin points as determined by the three methods are shown in Figure 10 by the numbered circles. Point (1) marks the approximate intersection of the distance arc from Monterey ($D = 2330$ nautical miles) and the adjusted distance arc from San Clemente Island ($D = 2574$ nautical miles) for an origin time of 0300Z 21 November 71 as derived from wave records at the two locations. Based on this intersection the arrival direction of the swell at Monterey was 297 degrees true. Points (2) and (3) represent origin times of 0330Z 21 November and 0600Z 21 November 71, respectively, and yield swell arrival directions at Monterey of $285.2^\circ T$ and $286.5^\circ T$, as determined by Methods Two and Three.

The source origin points for Methods Two and Three are quite close together (Figure 10). At first glance the origin point as determined by Method One may seem to be poor in relation to the other two; however, it should be noted that because of the small angle of intersection, a small change in the source distance determined from the f-t curves drawn from the spectral analysis of the wave records will change the north-south location of the intersection and the source point by a considerable amount. Clearly a more suitable baseline between sensors is needed. In view of these considerations, the agreement between the three methods applied to this storm is considered to be quite good.

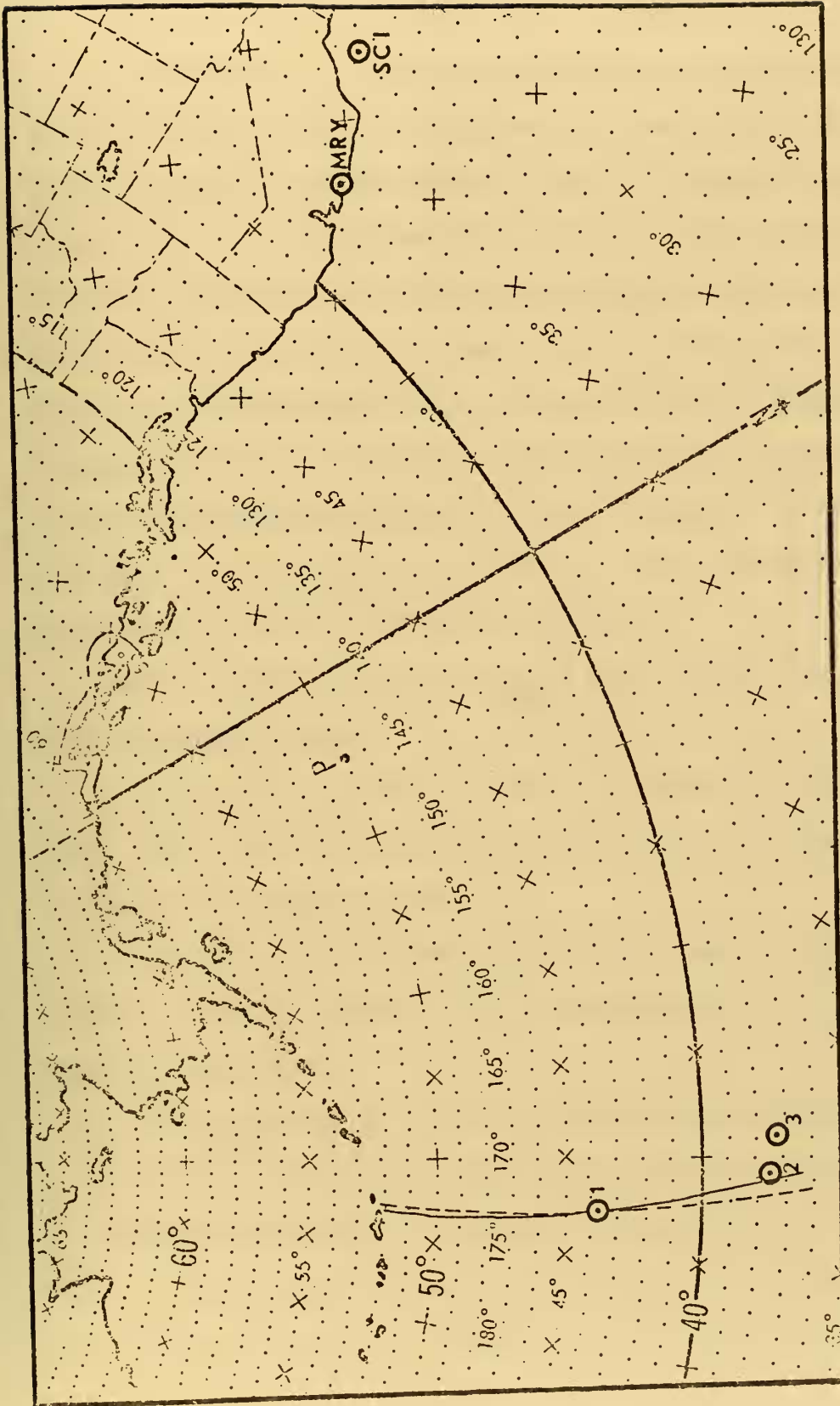


Figure 9: SWELL ORIGIN POINTS FOR STORM 3 AS DETERMINED BY METHODS ONE, TWO AND THREE.

B. COMPARISON OF METHODS TWO AND THREE FOR ALL STORMS

The comparisons of the swell source distance and origin time, and the arrival direction at Monterey, derived using Methods Two and Three for the five storms studied are shown in Table IV (obtained from Tables I and II). The table shows that the peak swell origin time differences vary from 15 minutes to 6 hours, and the distance differences from the origin point to Monterey vary from 37 to 140 nautical miles, with the exception of Storm 4A which had a 362 nautical mile difference. The differences in arrival direction of the peak swell at Monterey obtained from the two methods varied from 0.1 to 5.3 degrees. It may be noted that Method Two produced distances greater than those predicted from Method Three in five of the six cases studied.

Possible reasons for variability in the location of the origin using the two methods include:

1. Subjectivity in the fit of the $f-t$ curve to the spectral energy graph. This leads to some possible variation in the distance and time of origin of the observed swell.

2. Variability in the FNWC weather maps. Lack of data in a storm area may lead to an analysis that is unrepresentative of the actual surface pressure field present.

3. Poor estimates of the time of swell origin using Method Three.

Method Three, because of its somewhat subjective character, is prone to errors in determination of the origin point of the peak swell due to errors in estimating the correct time of origin. It is therefore appropriate to examine what the effect of a ± 12 hour and ± 24 hour time

error in the choice of time of origin of the peak swell will have on the swell arrival direction prediction at a distant coastal station such as Monterey. The results of this investigation for the five storms studied are shown in Table V. Clearly, an error in the predicted time of origin will have little effect on the arrival direction of ocean swell generated by storms at sea that are moving along approximate great-circle paths toward the coastal station. However, in the case of a storm such as Storm 5, where the path of the storm makes a large angle with the swell path to the coastal station, the effects of an error in time of origin prediction can be fairly large. It should be noted that from the results presented in Table IV, an error in estimation of the swell origin time in excess of 12 hours appears unlikely.

Table IV: COMPARISON OF RESULTS FROM METHODS TWO AND THREE

<u>Storm Number</u>	<u>Difference in Origin Time</u>	<u>Difference in Origin Distance</u>	<u>Difference in Arrival Direction</u>
1	4.0 Hours	103 naut. mi.*	0.6 °T
2	6.0	140	3.3
3	2.5	90*	1.3
4	3.0+	147*	1.0
4A	3.8	362*	5.3
5	0.2	37*	0.1

(+) Denotes Method Two gave origin time later than Method Three.

(*) Denotes Method Two gave origin distance greater than Method Three.

Table V: SWELL ARRIVAL DIRECTION AT MONTEREY RESULTING FROM
12 AND 24 HOUR ERROR IN ESTIMATING TIME OF ORIGIN

<u>Storm Number</u>	<u>-24</u>	<u>-12</u>	<u>0</u>	<u>+12</u>	<u>+24</u>
1	N.A.	304.7	306.7	305.8	206.8
2	307.6	307.2	305.2	308.4	308.6
3	285.7	286.1	285.2	286.5	289.9
4	301.7	300.0	300.0	297.2	292.8
4A	284.7	283.3	288.5	289.9	292.5
5	299.4	303.6	310.4	318.4	317.6

LIST OF REFERENCES

1. Barber, N. F., and F. Ursell, "The Generation and Propagation of Ocean Waves and Swell, I. Wave Periods and Velocities," Philosophical Transactions, Royal Society of London, v. 240, p. 527 to 560, 24 February 1948.
2. Blackman, R. B., and J. W. Tukey, "The Measurement of Power Spectra from the Point of View of Communications Engineering," Dover Publications, 1958.
3. Carstensen, L. P., Fleet Numerical Weather Facility, Technical Note No. 29. Some Effects of Sea Air Temperature Difference, Latitude and Other Factors on Surface Wind Geostrophic Wind Ratio and Deflection Angle, p. 1-9, March 1967.
4. Chang, D., "A Fortran Sub-Routine for the Great-Circle Distance Between Two Points and Bearings at the Points," Naval Research Laboratory Computer Note 32, 1 September 1969.
5. Lynch, T. J., Long Wave Study of Monterey Bay, Masters Thesis, Naval Postgraduate School, Monterey, California, September 1970.
6. Munk, W. H., G. R. Miller, F. E. Snodgrass and N. F. Barber, "Directional Recording of Swell from Distant Storms," Philosophical Transactions, Royal Society of London, v. 255, p. 505-584, 18 April 1963.
7. Pierson, W. J., and L. Moskowitz, "A Proposed Spectral Form for Fully Developed Wind Seas Based on the Similarity Theory of S. A. Kitaigorodskii," Journal of Geophysical Research, v. 69, p. 5181-5194, 15 December 1964.
8. Snodgrass, F. E., G. W. Groves, K. F. Hasselmann, G. R. Miller, W. H. Munk, and W. H. Powers, "Propagation of Ocean Swell Across the Pacific," Philosophical Transactions, Royal Society of London, v. 259, p. 431-497, 4 May 1966.
9. Thompson, W. C., "Swell and Storm Characteristics from Coastal Wave Records," American Society Civil Engineers, Proceedings, Twelfth Coastal Engineering Conference, p. 33-52, September 1970.

INITIAL DISTRIBUTION LIST

	No. Copies
1. Defense Documentation Center Cameron Station Alexandria, Virginia 22314	2
2. Library, Code 0212 Naval Postgraduate School Monterey, California 93940	2
3. Professor Warren C. Thompson Department of Oceanography Naval Postgraduate School Monterey, California 93940	5
4. Lieutenant M. H. Austin, Jr. USS Paul Revere (LPA-248) c/o FPO San Francisco 96601	2
5. Professor J. B. Wickham Department of Oceanography Naval Postgraduate School Monterey, California 93940	1
6. Department of Oceanography Naval Postgraduate School Monterey, California 93940	3
7. Lieutenant Commander Charles K. Roberts Department of Oceanography Naval Postgraduate School Monterey, California 93940	1
8. Oceanographer of the Navy The Madison Building 732 N. Washington Street Alexandria, Virginia 22314	1
9. Dr. Ned A. Ostenso Code 480D Office of Naval Research Arlington, Virginia 22217	1
10. Evelyn L. Pruit, Director Geography Programs, Code 414 Office of Naval Research Department of the Navy Washington, D. C. 20360	1

- | | | |
|-----|---|---|
| 11. | Commanding Officer
Environmental Prediction Research Facility
404 Franklin Street
Monterey, California 93940 | 1 |
| 12. | Commanding Officer
Fleet Numerical Weather Central
Monterey, California 93940 | 2 |
| 13. | Coastal Engineering Research Center
5201 Little Falls Road, N. W.
Washington, D. C. 20016 | 1 |
| 14. | Mr. Charles Fisher, Chief
Coastal Engineering Branch
U. S. Army Corps of Engineers
P. O. Box 2711
Los Angeles, California 90053 | 1 |
| 15. | Commanding Officer
San Francisco District
U. S. Army Corps of Engineers
100 McAllister Street
San Francisco, California 94102
Navigation and Shoreline Planning Section
Library | 2 |
| 16. | Coastal Engineering Branch
Planning Division
U. S. Army Engineering Division, South Pacific
630 Sansome Street
San Francisco, California 94111 | 1 |

DOCUMENT CONTROL DATA - R & D

(Security classification of title, body of abstract and indexing annotation must be entered when the overall report is classified)

1. ORIGINATING ACTIVITY (Corporate author) Naval Postgraduate School Monterey, California 93940	2a. REPORT SECURITY CLASSIFICATION Unclassified 2b. GROUP
---	---

3. REPORT TITLE
 Determination of the Deep Water Arrival Direction of Ocean Swell at a Coastal Station

4. DESCRIPTIVE NOTES (Type of report and, inclusive dates)
 Master's Thesis; March 1972

5. AUTHOR(S) (First name, middle initial, last name)
 Marshall Harlan Austin, Jr.

6. REPORT DATE March 1972	7a. TOTAL NO. OF PAGES	7b. NO. OF REFS 9
------------------------------	------------------------	----------------------

8a. CONTRACT OR GRANT NO. b. PROJECT NO. c. d.	9a. ORIGINATOR'S REPORT NUMBER(S) 9b. OTHER REPORT NO(S) (Any other numbers that may be assigned this report)
---	--

10. DISTRIBUTION STATEMENT
 Approved for public release; distribution unlimited.

11. SUPPLEMENTARY NOTES	12. SPONSORING MILITARY ACTIVITY Naval Postgraduate School Monterey, California 93940
-------------------------	---

13. ABSTRACT

Three previously unpublished methods for empirically determining deep-water swell direction were examined in this work: (1) triangulation using two widely separated wave sensors, (2) intersection using weather maps and a single wave sensor, and (3) swell point-source estimation from weather maps. The primary objective of each method was to identify a single point source of the swell train produced in an approaching cyclonic storm. Method (1) was not adequately tested, but results as applied to swell from one storm were favorable. Methods (2) and (3), applied to five selected North Pacific storms, gave close agreement on the swell origin time (15 minutes to 6 hours) and source point location (27 to 362 nautical miles), and on swell arrival direction at Monterey, California (0.1 to 5.3 degrees). Methods (1) and (2) give deep-water directions for swell trains that have already arrived, while Method (3) is a prediction method.

KEY WORDS

LINK A

LINK B

LINK C

ROLE

WT

ROLE

WT

ROLE

WT

Swell Propagation
Frequency-Time Graph
Swell Arrival Direction Prediction
Great-Circle Path
Great-Circle Distance
Great-Circle Azimuths

Duplicate

Thesis
A9715

133999

Austin

Determination of the
deep water arrival di-
rection of ocean swell
at a coastal station.

Th
A

Thesis
A9715
c.1

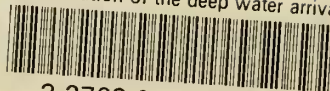
133999

Austin

Determination of the
deep water arrival di-
rection of ocean swell
at a coastal station.

thesA9715

Determination of the deep water arrival



3 2768 001 91073 0

DUDLEY KNOX LIBRARY